Check for updates

View Article Online
View Journal

ChemComm

Accepted Manuscript

This article can be cited before page numbers have been issued, to do this please use: K. Wang, Z. Fang, X. Huang, W. Feng, Y. Wang, B. Wang and P. Liu*, Chem. Commun.*, 2017, DOI: 10.1039/C7CC05112C.

Volume 52 | Number 1 | 4 January 2016 | Pages 1–216

ChemComm
Chemical Communications
www.rsc.org/chemcomm

ISSN 1359-7345

ROYAL SOCIETY OF CHEMISTRY

COMMUNICATION
Marilyn M. Olmstead, Alan L. Balch, Josep M. Poblet, Luis Echegoyen *et al.*
Reactivity differences of $Sc_3N@C_{2n}$ ($2n$ = 68 and 80). Synthesis of the first methanofullerene derivatives of $Sc_3N@D_{5h}$-C_{80}

175 YEARS

This is an Accepted Manuscript, which has been through the Royal Society of Chemistry peer review process and has been accepted for publication.

Accepted Manuscripts are published online shortly after acceptance, before technical editing, formatting and proof reading. Using this free service, authors can make their results available to the community, in citable form, before we publish the edited article. We will replace this Accepted Manuscript with the edited and formatted Advance Article as soon as it is available.

You can find more information about Accepted Manuscripts in the author guidelines.

Please note that technical editing may introduce minor changes to the text and/or graphics, which may alter content. The journal's standard Terms & Conditions and the ethical guidelines, outlined in our author and reviewer resource centre, still apply. In no event shall the Royal Society of Chemistry be held responsible for any errors or omissions in this Accepted Manuscript or any consequences arising from the use of any information it contains.

ROYAL SOCIETY OF CHEMISTRY

rsc.li/chemcomm

View Article Online
DOI: 10.1039/C7CC05112C

Journal Name

COMMUNICATION

Enhanced Selectivity of Methane Production for Photocatalytic Reduction by Piezoelectric Effect

Received 00th January 20xx,
Accepted 00th January 20xx

DOI: 10.1039/x0xx00000x

www.rsc.org/chemcomm

Kaiqiang Wang, Zhibin Fang, Xueyan Huang, Wenhui Feng, Yaozhu Wang, Bo Wang, and Ping Liu*

Under simultaneous irradiation of full arc light and ultrasonic, the photo-generated electrons are brought together by piezoelectric potential, thus dense electrons involve the reduction of carbon dioxide on the surface of piezoelectric semiconductor, resulting in the improved selectivity of methane production to a greater degree.

Reduction of CO_2 has attracted much attention under the current background of the depletion of fossil resources and the increase of emissions of CO_2. The photocatalytic conversion of CO_2 using solar energy is the most promising route for the transformation of CO_2 to specific fuels and chemicals.[1] However, one of the severe problems in limiting practical applications of CO_2 photoreduction technology is the low selective yields of particular products. To solve this issue, much effort has been made, such as loading co-catalysts,[2-7] doping ions or metals,[8] and optimizing synthesized methods of catalysts.[9, 10] Among various treatment solutions, loading co-catalysts is the most attractive technology for its green and facile feature. It has been demonstrated that the photocatalytic selectivity of particular products can be influenced by loading co-catalysts.[2-7] For example, methane was selectively produced by loading metallic copper acted as electron traps resulting in an increased probability of multiple electrons reactions.[2] The method of loading co-catalysts has shown improved effect greatly, while the high cost and stringent operation on loading co-catalysts may restrain the practical applications at industrial level. The demand for new low-cost and effortless technology in enhancing the selective yields of particular chemicals is rapidly increasing.

Piezoelectrics are a class of functional materials which have great potential in many fields. Under applied deformation, there is a separation between the positive and negative charge centers that results in an electric field.[11] The origin of the non-zero electric field is a break in the inversion symmetry which lead to electric dipoles within the material, the strength of which changes as the material is strained.[11] As already reported, the piezopotential can effectively influence charge transport resulting in significantly enhanced optoelectronic performances. This is known as the piezophototronic effect presence in piezoelectric-semiconductor materials.[12-19] It is generally accepted that objects will migrate and gather together with a specific direction when confronted with a force, and so do the photo-generated electrons and holes. If the photo-generated carriers are introduced into a piezoelectric field, their movements may be influenced by the piezopotential formed in piezoelectric field. Similar to the above-mentioned impact of metallic copper, the local density of photo-generated electrons may be increased by the oriented driving effect of piezopotential, which would be beneficial for the multi-electron reactions.

Herein, for the first time, we establish a novel fundamental piezo-photocatalytic mechanism that can selectively convert carbon dioxide to methane under both photonic and mechanical energy through coupling the piezoelectric and photocatalytic properties of ZnO nanorods. With the assistance of piezopotential, the selectivity of methane production is improved. Such an economic and green method of energy treatment shows greatly potential applications in harvesting mechanical energy in the natural environment, such as noise, vibration, wind, tide, sonic wave and atmospheric pressure.[18, 20-23]

The hydrothermal or solvothermal methods are low-cost and convenient, yet robust methods for the synthesis and morphological transformation of many nanostructures.[24] In the current study, ZnO nanorods were prepared by a solvothermal method.[25] The XRD pattern of pure ZnO is given in (Fig. S1a, ESI†). All the diffraction peaks can be well-indexed to hexagonal phase of ZnO (space group: P63mc) crystal. As shown in the original SEM image (Fig. 1a), straight and smooth rods with ca. 20-30 nm in diameter and 0.5–1 µm in length are synthesized successfully. The HRTEM image in Fig. 1b obviously

---

Research Institute of Photocatalysis, State Key Laboratory of Photocatalysis on Energy and Environment, College of Chemistry, Fuzhou University, Fuzhou 350002, P. R. China. E-mail: liuping@fzu.edu.cn;
Tel & Fax number: +86-591-83779239.

† Electronic Supplementary Information (ESI) available: Sample preparation, evolution tests of gas-phase products, detailed characterization, and Fig. S1 – S8. See DOI: 10.1039/x0xx00000x

View Article Online
DOI: 10.1039/C7CC05112C

confirm that ZnO sample grow along the direction of [0 0 0 1] plane forming a rod-like structure with a typical lattice of 0.26 nm. The optical absorbance of ZnO NRs is measured by UV-visible absorption spectra (Fig. S2, ESI†). ZnO NRs have a wide-band gap (3.15 eV at room temperature) and almost do not absorb visible light. Hence, ultraviolet light is essential for the optical irradiation.

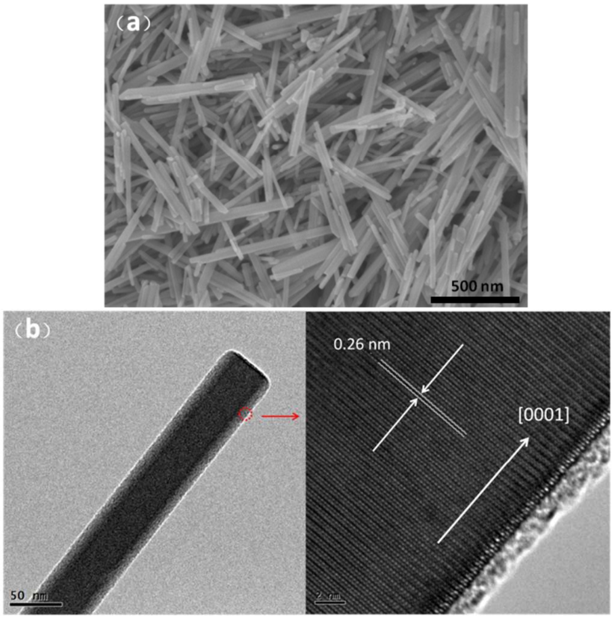

Fig. 1 Morphology of the solvothermally synthesized ZnO NRs with (a) SEM image and (b) HRTEM image.

To demonstrate the effect of ultrasonic irradiation on the photocatalytic performance of ZnO NRs, the reductive reaction of CO_2 is evaluated respectively under ultrasonic irradiation (40 kHz, 50 W), full arc（UV-Vis）light irradiation, and simultaneous irradiation of full arc light and ultrasonic. In our approach, the piezopotential in ZnO NRs is periodically altered by applying ultrasonic wave, the schematic diagram of reaction device is illustrated in (Fig. S3, ESI†). In our experimental conditions, CO and CH_4 are dectected as the gas-phase products of reducing CO_2. As shown in Fig. 2a, the productive rates of CO and CH_4 are 0.492 μl·h^{-1} and 0.0391 μl·h^{-1} respectively under full arc light irradiation (L). While under the condition of simultaneous irradiation of full arc light and ultrasonic (L+S), the corresponding values turn to 0.714 μl·h^{-1} and 0.112 μl·h^{-1} respectively. Under the condition of L+S, the yields of CO and CH_4 are increased, yet the production of CH_4 rises to a greater degree. Compared with L condition, the selectivity of methane production is increased from 7.36% to 13.56% under the condition of L+S as demonstrated in Fig. 2b, which almost increases doubled. However, as a piezoelectrochemical catalyst, only using ultrasonic irradiation (S), the productive rates of CO and CH_4 are limited, which below the detection limit of the chromatography.

The photocatalytic reduction of carbon dioxide is usually thought to be a multiple electrons reaction. During the photoreduction process, eight electrons are required in the formation of each CH_4 molecule,[26-30] and only two electrons are needed for each CO molecule evolution,[1, 28-31] which means the transformation of CH_4 need more electrons than that of CO. In our experiment, CO is detected as the major gas-phase product while CH_4 as the minor product. Therefore, the photocatalytic reduction of CO_2 to CO may be a dynamic favored process in the present system.[32] In order to demonstrate the reduction of CO_2 is induced by photocatalytic progress, we carry out several blank experiments under L and L+S irradiation. CO and CH_4 are negligibly detected in the absence of the following three substances individually, which are catalyst, full arc light irradiation and CO_2. These related results confirm that CO and CH_4 are formed by the photocatalytic reduction of CO_2 using ZnO NRs.

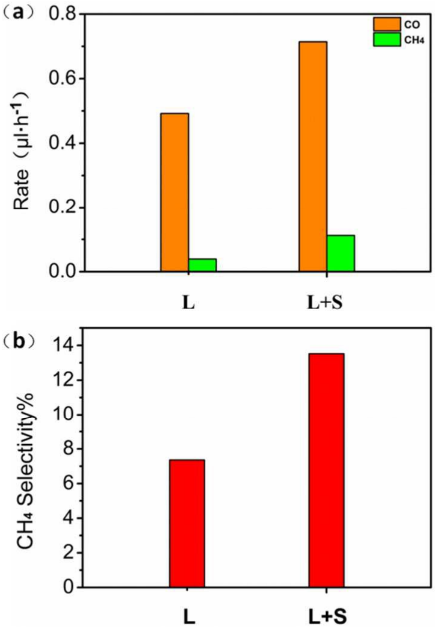

Fig. 2 Reduction of CO_2 by 20 mg ZnO NRs with (a) productive rates of CO and CH_4 and (b) selective percentage of CH_4 under different conditions.

When illuminated by full arc light with sufficient photonic energy and appropriate wavelength, photo-generated electrons (e^-) and holes (h^+) are created on the surface of ZnO NRs. The electrons in the valence band are excited to the conduction band, leaving an equal number of holes in the valence band. As a periodic force is applied on ZnO, the nanorods are forced to bend and form a piezoelectric field across its width with negative piezopotential on the compressive strain region (blue) and positive piezopotential on the tensile strain region (red) as shown in the top left of Fig. 3.[33] The piezoelectric field provides a driving force for attracting electrons to migrate to the positive surface and the holes flow away to the negative surface,[33, 34] thus causes the internal movement of the photo-generated carriers with a specific orientation. From the infrared spectra and Raman spectroscopy of ZnO NRs (Fig. S4 and Fig. S5, ESI†), no characteristic absorption peaks of the organic residues are detected, which demonstrates that the surface of ZnO are clean. Holes directly oxidize H_2O molecules and the electrons react with CO_2, generating O_2, CO and CH_4. This piezo-driven carrier migration reduces the recombination rate of photo-generated electrons and holes, and more carriers migrate to the surface of ZnO NRs, hence, the yields of CO and CH_4 are increased. Increasing the density of electrons can indeed improve the selectivity of CH_4 production which has been testified by experiments (Fig. S6 and Fig. S7, ESI†). The migration of the photo-generated carriers to the surface along the opposite direction by piezoelectric potential increases the local density of electrons, which is beneficial for the production of CH_4 requiring eight electrons to be transformed.

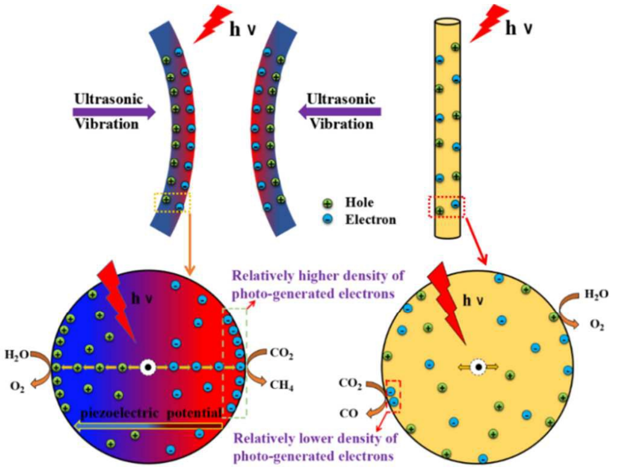

Fig. 3 Schematic diagram illustrating the distribution of photo-generated carriers in ZnO NRs under L and L+S condition.

For sole ZnO material, the decay lifetime of carriers is in nanosecond scale,[35, 36] while the switching frequency of the bending direction for the generated piezoelectric field caused by the applied periodic ultrasound is 25 μs (40 kHz). The generation and movement speed of photo-generated carriers is obviously faster than that of direction alternation of the piezoelectric field. For one carrier reaction, the migrated and reactive progress can be regarded in a static electric field with a constant intensity and direction. When the force direction change to the other side, the essence of this chemical reaction has not changed, just the properties of surface charge become opposite.

For photocatalytic reaction, the absorption of reactants and desorption of products are conducted on the local area of catalyst surface. While under the full arc light irradiation without the assistance of piezopotential, no driving force make the photo-generated electrons migrate to the surface of ZnO NRs directionally, causing a relatively lower density of electrons on the local surface area compared with L+S condition (as shown in the bottom right of Figure 3). As a periodic force applied on ZnO NRs, oriented migration of electrons caused by piezoelectric potential is essential to increase the local electron density that improves the selectivity of methane. With the assistance of piezopotential, the sparse electrons difficult to reach the reductive degree of yielding CH_4 would be assembled together so that the production of CH_4 increases.

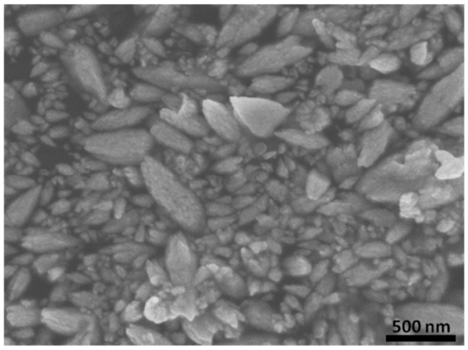

Fig. 4 SEM image of ZnO nanoparticles.

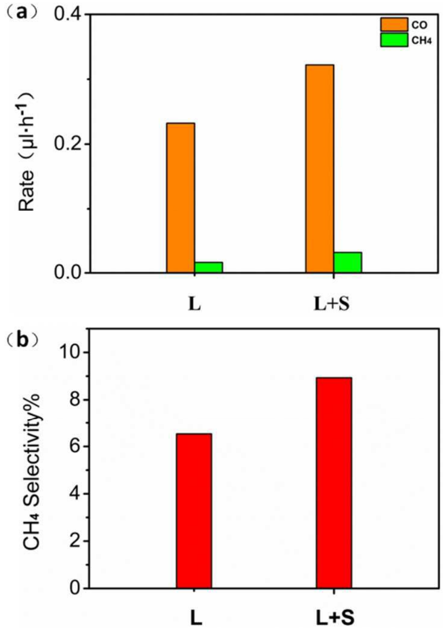

Fig. 5 Reduction of CO_2 by 20 mg ZnO particles with (a) productive rates of CO and CH_4 and (b) selective percentage of CH_4 under different conditions of non-rod shaped ZnO.

Compared with ZnO NRs, wurtzite ZnO nanoparticles (Fig. S1b, ESI†) with non-rod shapes (Fig. 4) show lower selectivity for methane production. As shown in Fig. 5a, the productive rates of CO and CH_4 are 0.232 $\mu l \cdot h^{-1}$ and 0.0162 $\mu l \cdot h^{-1}$ respectively under L condition. While under the condition of L+S, the corresponding values increase to 0.322 $\mu l \cdot h^{-1}$ and 0.0316 $\mu l \cdot h^{-1}$ respectively. Compared with L condition, the selectivity of methane production is increased from 6.53% to 8.94% under the condition of L+S (Fig. 5b). The ZnO NRs synthesized by solvothermal method not only produce more gas-phase products but also have a higher selectivity of methane production under the condition of L+S. The large amounts of ZnO nanoparticles have no uniform c-axis direction, which is similar to the polycrystalline structure. Fibers with longer lengths exhibit a greater bending curvature than that of shorter fiber lengths when under the same

View Article Online
DOI: 10.1039/C7CC05112C

applied force in a vibration event.[37] Due to this property, ZnO NRs built up a higher piezopotential than particles with equal mechanical vibration. It is for this reason that non-rod shaped ZnO nanoparticles exhibit relatively limited selectivity for reducing CH_4. In addition, the photocatalytic performance and the selectivity of CH_4 production have not been improved by anatase TiO_2 (none piezoelectric properties) under L+S condition (Fig. S8, ESI†). These results further confirm that the enhancement of photocatalytic efficiency of ZnO arises from the piezo-assistance.

In summary, a new fundamental piezo-photocatalytic mechanism is demonstrated. Photo-generated carriers can be enriched on the local surface of ZnO NRs by the piezoelectric potential formed in piezoelectric semiconductor, hence the local density of photo-generated electrons and the selectivity of methane production are increased. Although the improved degree is not obvious in our work, it can present a possibility for using piezoelectric effect to enhance the multi-electron reaction. This practice not only realizes the energy recycling by means of energy wastes such as noise or stray vibrations from the environment, but also makes contribution to environmental sustainability.

Notes and references

1 Q. Zhai, S. Xie, W. Fan, Q. Zhang, Y. Wang, W. Deng and Y. Wang, Angew. Chem., Int. Ed., 2013, **52**, 5776-5779.
2 Y. Li, W.-N. Wang, Z. Zhan, M.-H. Woo, C.-Y. Wu and P. Biswas, Appl. Catal., B, 2010, **100**, 386-392.
3 W. N. Wang, W. J. An, B. Ramalingam, S. Mukherjee, D. M. Niedzwiedzki, S. Gangopadhyay and P. Biswas, J. Am. Chem. Soc., 2012, **134**, 11276-11281.
4 T. Yui, A. Kan, C. Saitoh, K. Koike, T. Ibusuki and O. Ishitani, *ACS Appl. Mat. Interfaces*, 2011, **3**, 2594-2600.
5 M. Manzanares, C. Fàbrega, J. Oriol Ossó, L. F. Vega, T. Andreu and J. R. Morante, Appl. Catal., B, 2014, **150-151**, 57-62.
6 H. Yamashita, Y. Fujii, Y. Ichihashi, S. G. Zhang, K. Ikeue, D. R. Park, K. Koyano, T. Tatsumi and M. Anpo, *Catal. Today.*, 1998, **45**, 221-227.
7 K. Kočí, K. Matějů, L. Obalová, S. Krejčíková, Z. Lacný, D. Plachá, L. Čapek, A. Hospodková and O. Šolcová, Appl. Catal., B, 2010, **96**, 239-244.
8 L. Jia, J. Li and W. Fang, *Catal. Commun.*, 2009, **11**, 87-90.
9 W. Jiang, X. Yin, F. Xin, Y. Bi, Y. Liu and X. Li, *Appl. Surf. Sci.*, 2014, **288**, 138-142.
10 K. Ikeue, H. Yamashita, M. Anpo and T. Takewaki, *The J. Phys. Chem. B.*, 2001, **105**, 8350-8355.
11 M. B. Starr and X. Wang, *Nano Energy*, 2015, **14**, 296-311.
12 J. Yang, J. Chen, Y. Liu, W. Yang, Y. Su and Z. L. Wang, *ACS nano*, 2014, **8**, 2649-2657.
13 Y. Liu, S. Niu, Q. Yang, B. D. Klein, Y. S. Zhou and Z. L. Wang, Adv. Mater., 2014, **26**, 7209-7216.
14 W. Wu, C. Pan, Y. Zhang, X. Wen and Z. L. Wang, *Nano Today*, 2013, **8**, 619-642.
15 Z. L. Wang, Adv. Mater., 2012, **24**, 4632-4646.
16 Z. L. Wang, *Nano Today*, 2010, **5**, 540-552.
17 Z. L. Wang, Adv. Mater., 2007, **19**, 889-892.
18 X. Wang, J. Song, J. Liu and Z. L. Wang, *Science*, 2007, **316**, 102-105.
19 Z. L. Wang and J. Song, *Science*, 2006, **312**, 242-246.
20 Y. Yang, K. C. Pradel, Q. Jing, J. M. Wu, F. Zhang, Y. Zhou, Y. Zhang and Z. L. Wang, *ACS nano*, 2012, **6**, 6984-6989.
21 Y. Xie, S. Wang, L. Lin, Q. Jing, Z.-H. Lin, S. Niu, Z. Wu and Z. L. Wang, *ACS nano*, 2013, **7**, 7119-7125.
22 S. Bai, L. Zhang, Q. Xu, Y. Zheng, Y. Qin and Z. L. Wang, *Nano Energy*, 2013, **2**, 749-753.
23 S. Xu, Y. Wei, J. Liu, R. Yang and Z. L. Wang, Nano Lett., 2008, **8**, 4027-4032.
24 O. Carp, Prog. Solid. State. Ch., 2004, **32**, 33-177.
25 Q. Wang, B. Geng, S. Wang, Y. Ye and B. Tao, Chem. Commun., 2010, **46**, 1899-1901.
26 S. C. Yan, S. X. Ouyang, J. Gao, M. Yang, J. Y. Feng, X. X. Fan, L. J. Wan, Z. S. Li, J. H. Ye, Y. Zhou and Z. G. Zou, Angew. Chem., Int. Ed., 2010, **49**, 6400-6404.
27 Q. Liu, Y. Zhou, J. Kou, X. Chen, Z. Tian, J. Gao, S. Yan and Z. Zou, J. Am. Chem. Soc., 2010, **132**, 14385-14387.
28 E. E. Benson, C. P. Kubiak, A. J. Sathrum and J. M. Smieja, Chem. Soc. Rev., 2009, **38**, 89-99.
29 A. J. Morris, G. J. Meyer and E. Fujita, *Accounts. Chem. Res.*, 2009, **42**, 1983-1994.
30 Y. Hori, in *Modern aspects of electrochemistry*, Springer, 2008, pp. 89-189.
31 G. Dong and L. Zhang, *J. Mater. Chem.*, 2012, **22**, 1160-1166.
32 S. Zhou, Y. Liu, J. Li, Y. Wang, G. Jiang, Z. Zhao, D. Wang, A. Duan, J. Liu and Y. Wei, Appl. Catal., B, 2014, **158-159**, 20-29.
33 X. Xue, W. Zang, P. Deng, Q. Wang, L. Xing, Y. Zhang and Z. L. Wang, *Nano Energy*, 2015, **13**, 414-422.
34 D. Tiwari, S. Dunn and Q. Zhang, *Mater. Res. Bull.*, 2009, **44**, 1219-1224.
35 X. Wang, G. Liu, Z. G. Chen, F. Li, L. Wang, G. Q. Lu and H. M. Cheng, Chem. Commun., 2009, DOI: 10.1039/b904668b, 3452-3454.
36 J. B. Baxter and C. A. Schmuttenmaer, The J. Phys. Chem. B., 2006, **110**, 25229-25239.
37 J. Song, J. Zhou and Z. L. Wang, Nano Lett., 2006, **6**, 1656-1662.